

Effective Computational Modeling of Constitutional Isomerism and Aggregation States of Explicit Solvates of Lithiated Phenylacetonitrile

Paul R. Carlier^{*,†} and Jeffry D. Madura[‡]

Department of Chemistry, Virginia Tech, Blacksburg, Virginia 24060, and
Department of Chemistry and Biochemistry, Duquesne University, Pittsburgh, Pennsylvania 15282

pcarlier@vt.edu

Received January 28, 2002

We present the first calculations which accurately account for the position of metalation and aggregation state of lithiated nitriles. *Solvation is found to be a key determinant of structure.* Five known solvates of lithiated phenylacetonitrile were examined computationally to determine the minimum level of theory required to reproduce the observed X-ray and multinuclear NMR structures. In all cases Hartree–Fock 3-21G energies of explicit solvates calculated at PM3 geometries correctly predict the observed N-lithiated constitutional isomer. Selected density functional theory (B3LYP/6-31+G**/PM3) energy calculations reproduce this trend. We also show that 3-21G/PM3 calculations which do not include explicit solvent molecules, or which include water as a model for diethyl ether, may lead to incorrect predictions of the preferred constitutional isomer. 3-21G/PM3 energies also adequately account for observed aggregation states of the TMEDA, diethyl ether, and THF solvates. Finally, calculations of THF-solvated monomers up to the B3LYP/6-31+G**/B3LYP/6-31+G* level indicate a significant (6.8 kcal/mol) preference for N-lithiation.

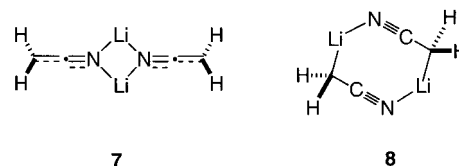
Introduction

The structure of lithiated nitriles has attracted considerable interest from both theoreticians^{1–4} and experimentalists.^{5–16} A central issue in these studies is which constitutional isomer is preferred: N-lithiated or C-lithiated (Chart 1).

Chart 1. Ab Initio Energies of N- and C-Lithiated Nitriles

		ΔH (kcal/mol)	basis
1 (R = H)	4 (R = H)	-9.8	MP2/6-31G*
2 (R = NH ₂)	5 (R = NH ₂)	-8.8	//6-31G*
3 (R = Ph)	6 (R = Ph)	-0.40	3-21+G*

Chart 2. Cyclic Dimers of Lithiated Acetonitrile



* To whom correspondence should be addressed.

[†] Virginia Tech.

[‡] Duquesne University.

(1) Kaneti, J.; von R. Schleyer, P.; Clark, T.; Kos, A. J.; Spitznagel, G. W.; Andrade, J. G.; Moffat, J. B. *J. Am. Chem. Soc.* **1986**, *108*, 1481–1492.

(2) Raabe, G.; Zobel, E.; Fleischhauer, J.; Gerdes, P.; Mannes, D.; Müller, E.; Enders, D. *Z. Naturforsch.* **1991**, *46a*, 275–288.

(3) Koch, R.; Wiedel, B.; Anders, E. *J. Org. Chem.* **1996**, *61*, 2523–2529.

(4) Strzalko, T.; Seyden-Penne, J.; Wartski, L.; Corset, J.; Castella-Ventura, M.; Froment, F. *J. Org. Chem.* **1998**, *63*, 3287–3294.

(5) Boche, G.; Marsch, M.; Harms, K. *Angew. Chem., Int. Ed. Engl.* **1986**, *25*, 373–374.

(6) Boche, G.; Harms, K.; Marsch, M. *J. Am. Chem. Soc.* **1988**, *110*, 6925–6926.

(7) Zarges, W.; Marsch, M.; Harms, K.; Boche, G. *Angew. Chem., Int. Ed. Engl.* **1989**, *28*, 1392–1394.

(8) Lambert, C.; Schleyer, P. v. R.; Pieper, U.; Stalke, D. *Angew. Chem., Int. Ed. Engl.* **1992**, *31*, 77–79.

(9) Hiller, W.; Frey, S.; Strähle, J.; Boche, G.; Zarges, W.; Harms, K.; Marsch, M.; Wollert, R.; Dehnicke, K. *Chem. Ber.* **1992**, *125*, 87–92.

(10) Enders, D.; Kirchhoff, J.; Gerdes, P.; Mannes, D.; Raabe, G.; Runsink, J.; Boche, G.; Marsch, M.; Ahlbrecht, H.; Sommer, H. *Eur. J. Org. Chem.* **1998**, *63*, 3–72.

(11) Langlotz, I.; Marsch, M.; Harms, K.; Boche, G. *Z. Kristallogr.—New Cryst. Struct.* **1999**, *214*, 509–510.

(12) Ledig, B.; Marsch, M.; Harms, K.; Boche, G. *Z. Kristallogr.—New Cryst. Struct.* **1999**, *214*, 511–512.

(13) Carlier, P. R.; Lucht, B. L.; Collum, D. B. *J. Am. Chem. Soc.* **1994**, *116*, 11602–11603.

(14) Carlier, P. R.; Lo, C. W. S. *J. Am. Chem. Soc.* **2000**, *122*, 12819–12823.

(15) Croisat, D.; Seyden-Penne, J.; Strzalko, T.; Wartski, L.; Corset, J.; Froment, F. *J. Org. Chem.* **1992**, *57*, 6435–6447.

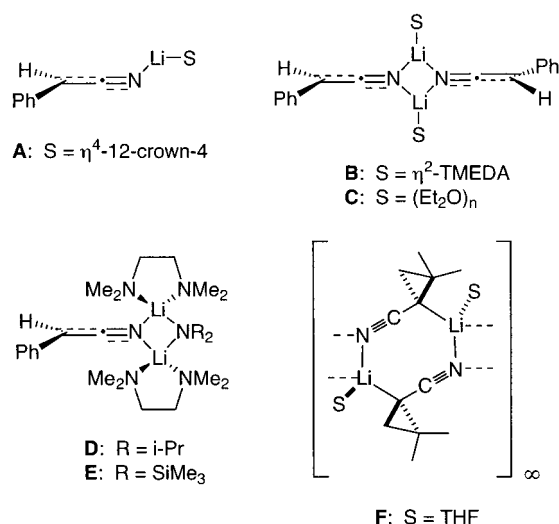
(16) Strzalko, T.; Seyden-Penne, J.; Wartski, L.; Corset, J.; Castella-Ventura, M.; Froment, F. *J. Org. Chem.* **1998**, *63*, 3295–3301.

At the outset, it would appear that this preference might be affected by a number of factors, including the identity of the substituent (R), the aggregation state, and solvation. To date, ab initio calculations on unsolvated lithiated acetonitrile (**1**, **4**),^{1,2} aminoacetonitrile (**2**, **5**),² and phenylacetonitrile (**3**, **6**)⁴ have shown a preference for nonclassical C-lithiated structures **4–6** over the N-lithiated structures **1–3**. MNDO calculations of water solvates (mono, di, tri) of **1** and **4** also indicate an approximate 18 kcal/mol preference for the C-lithiated isomer **4**; studies of lithiated acetonitrile dimers and their water solvates (di, tetra) suggest a 35–45 kcal/mol preference for head-to-tail (C,N)-bridged dimer **8** relative to N-lithiated dimer **7** (Chart 2).¹

Schleyer took pains to point out that MNDO overestimates C–Li bond energies, and that consequently dimers **7** and **8** (and their solvates) may be very close in

Table 1. Calculated Bond Lengths and Angles for Unsolvated Lithiated Phenylacetonitrile Constitutional Isomers 3 and 6^a

	N-lithiated isomer 3				C-lithiated isomer 6			
	PM3	3-21G	3-21+G*	6-31G*	PM3	3-21G	3-21+G*	6-31G*
Bond Lengths (Å)								
Li–N	1.803	1.745	1.773	1.777	4.132	2.798	2.524	2.401
C1–N	1.206	1.177	1.170	1.174	1.166	1.155	1.153	1.156
C1–C2	1.342	1.337	1.342	1.345	1.416	1.403	1.391	1.397
Li–C2					2.075	2.088	2.148	2.150
Li–C1					3.112	2.255	2.127	2.083
Li–C3					2.455	2.234	2.285	2.346
Li–C4					2.511	2.386	2.398	2.448
Bond Angles (deg)								
C2–C1–N	178.4	179.7	179.7	179.9	178.3	170.5	167.9	164.3
C1–N–Li	178.6	178.5	"linear"	177.8				
Li–C1–C2					33.1	64.8	71.8	73.4
Li–C2–C3					86.0	65.1	76.2	78.7

^a Calculated 3-21+G* bond lengths were taken from ref 4.**Chart 3. Representative X-ray and Solution NMR Structures of Lithiated Nitriles**

energy.¹ Nevertheless, it must be concluded that the calculations published to date cannot account for the general preference for nitrile N-lithiation established both in the solid state^{5,7–12} and in the solution phase¹³ (Chart 3).

In this paper, we revisit the five structures of lithiated phenylacetonitrile (**A–E**) in which the position of metalation and aggregation state have been unambiguously established by X-ray crystallography or observation of ⁶Li–¹⁵N scalar coupling. PM3 geometries of the observed explicit solvates and their hypothetical constitutional isomers were determined. In all cases, Hartree–Fock (HF) 3-21G energies calculated at PM3 geometries correctly predict the observed N-lithiated constitutional isomer to be the most stable, and accurately model aggregation equilibria. Selected density functional theory (DFT; B3LYP/6-31+G*) energy calculations reproduce this trend. We also show that 3-21G/PM3 calculations which do not include explicit solvent molecules, or which include water as a model for diethyl ether, may lead to incorrect predictions of the preferred constitutional isomer. Finally, the structure of lithiated phenylacetonitrile in THF solution is addressed using full geometry optimization at the semiempirical (PM3), HF (3-21G), and DFT (B3LYP/6-31+G*) levels.

Modeling of a Known N-Lithiated Monomer (**A**)

Monomeric lithiated phenylacetonitrile has been detected in the solution phase using cryoscopic,¹⁷ IR/raman,^{4,15} and multinuclear NMR¹⁴ techniques. However, the position of metalation is known with certainty in only one case, the X-ray crystal structure of the 12-crown-4 solvate of **3** (structure **A** of Chart 3).¹¹ This structure features N-lithiation, a Li–N–C1 angle of 158.7°, and η^4 -coordination of the crown ether. To see whether the structure of the PhCHCNLi unit in **3** (η^4 -12-crown-4) could be adequately modeled without taking solvation into account, we performed calculations on lithiated phenylacetonitrile constitutional isomers **3** and **6**. The structures of unsolvated **3** and **6** have been studied previously at the 3-21G//3-21G and 3-21+G*//3-21+G* levels.⁴ We repeated the geometry optimization at the 3-21G level, and also performed optimizations at the PM3 and 6-31G* levels. Other than a slight decrease in the Li–N and C1–N bond lengths, there is little change in the structure of N-lithiated isomer **3** as the level of the calculation increases from PM3 to 6-31G* (Table 1).

In contrast, there are significant changes in the geometry of the C-lithiated species **6** as the level of the calculation increases (Figure 1).

At the PM3 level an η^3 -benzylolithium-type structure¹⁸ is seen that features close contact of Li to *ipso* carbon C3 (2.455 Å) and *ortho* carbon C4 (2.511 Å), but that exhibits no significant Li–N contact (4.132 Å). However, at HF levels an η^5 -species is seen that retains close Li–C3 and Li–C4 contacts, but features a decidedly nonlinear C2–C1–N angle and significant Li–C1 and Li–N contact (164° and 2.083 and 2.401 Å, respectively, at 6-31G*).

This structural variation in unsolvated **6** serves to equalize the energies of the constitutional isomers (Table 2).

At the PM3 geometry, a 7–11 kcal/mol preference for N-lithiation is indicated on the basis of PM3, 3-21G, 6-31G*, and B3LYP/6-31+G* energies. However, at HF geometries the preference for N-lithiation diminishes, and at 6-31G*//6-31G*, a 1.2 kcal/mol preference for the C-lithiated isomer **6** emerges. This slight preference is reversed at the B3LYP/6-31+G*//6-31G* level, suggesting little energy difference between unsolvated **3** and **6**. It

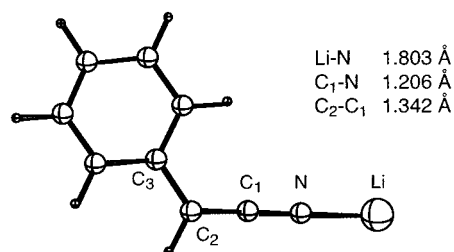
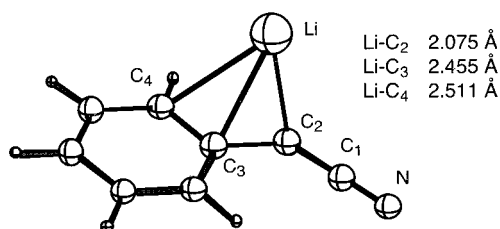
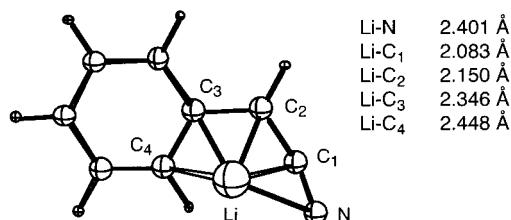
(17) Bauer, W.; Seebach, D. *Helv. Chim. Acta* **1984**, *67*, 1972–1988.(18) Anders, E.; Koch, R.; Freunsch, P. *J. Comput. Chem.* **1993**, *14*, 1301–1312.

Table 2. Energetic Preference for Unsolvated N-Lithiated Constitutional Isomer 3

method/basis//geometry	$E(3) - E(6)$ (kcal/mol)	method/basis//geometry	$E(3) - E(6)$ (kcal/mol)
PM3//PM3	-9.36	3-21G//3-21G	-5.63
3-21G//PM3	-11.15	3-21+G*//3-21+G* ^a	0.40
6-31+G*//PM3	-7.00	6-31G*//6-31G*	1.19
B3LYP/6-31+G*//PM3	-9.90	B3LYP/6-31+G*//6-31G*	-0.87

^a 3-21+G* energies were taken from ref 4.**Table 3. Observed Bond Lengths and Angles for A and Calculated Relative Energies,^a Bond Lengths, and Bond Angles for 3·(η^4 -12-crown-4) and Hypothetical C-Metalated Isomer 6·(η^4 -12-crown-4)**

	3·(η^4 -12-crown-4) actual (A)	3·(η^4 -12-crown-4) calcd	calcd - exptl	6·(η^4 -12-crown-4) calcd
PM3 energy		0		9.65
3-21G//PM3 energy		0		6.82
B3LYP/6-31+G*//PM3 energy		0		6.80
bond lengths (Å)				
Li-N	1.952(7)	1.845	-0.108	3.528
N-C1	1.168(5)	1.196	0.028	1.169
C1-C2	1.384(6)	1.353	-0.032	1.424
Li-C2				2.11
Li-C1				2.677
Li-C3				3.035
av Li-O	2.118	2.188	0.070	2.177
bond angles (deg)				
C2-C1-N	178.0	178.5	0.5	178.3
Li-C1-C2				51.5
Li-C2-C3				115.2
C1-N-Li	158.7	176.5	17.8	

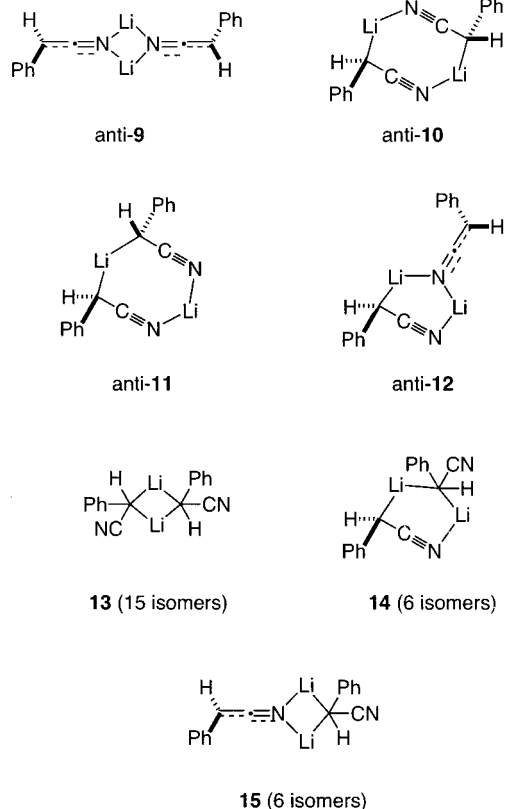
^a In kilocalories per mole.**3** (PM3 Geometry, C_s symmetry)**6** (PM3 Geometry)**6** (6-31G* Geometry)**Figure 1.** Equilibrium geometries and selected bond lengths of unsolvated monomers **3** and **6**.

would be difficult therefore to attribute the observation of structure **A** in the solid state to an intrinsic preference of *unsolvated* lithiated phenylacetonitrile for N-lithiation.

To determine whether the observed N-lithiation is the consequence of solvation or crystal packing, a study of the explicit 12-crown-4 solvate was undertaken. So we could study fully solvated monomers and dimers in a reasonable amount of time, we decided to employ a semiempirical method for geometry optimization. The PM3 method is known to be superior to MNDO for approximating the structures of organolithium compounds.¹⁸ PM3 geometries have previously been shown to model well the crystallographically determined structures of TMEDA-solvated dimers of lithiated phenylacetonitrile (structures **B** and **D** of Chart 3, *vide infra*),³ as well as those of TMEDA-solvated sulfones, sulfoxides, and dithianes.¹⁹ The PM3 geometries of explicit solvates of lithium enolate monomers, dimers, and trimers also show excellent agreement with the corresponding B3LYP geometries.²⁰ We thus performed a PM3 geometry optimization on **3**·(η^4 -12-crown-4) and on its hypothetical C-metalated isomer **6**·(η^4 -12-crown-4). The geometrical parameters for **3**·(η^4 -12-crown-4) adequately match those determined for **A** by crystallography (Table 3).

The largest deviations from the X-ray data are seen in the Li-N bond length (-0.108 Å), the average Li-O bond length (+0.070 Å), and the C1-N-Li bond angle (+17.8°). C-lithiated constitutional isomer **6**·(η^4 -12-crown-4) reverts from the η^3 -benzylolithium-type structure seen for unsolvated **6** (at the PM3 geometry) to a classical η^1 -C-lithiated structure (Li-C3 = 3.035 Å). Apparently, the crown ether oxygens are more effective ligands for lithium than the π bond of the phenyl substituent. Comparison of the PM3 energies of **3**·(η^4 -12-crown-4) and **6**·(η^4 -12-crown-4) suggest that the N-lithiated structure will be most stable, consistent with the X-ray data. But since semiempirical methods are known to have poor accuracy for thermochemical determinations, HF ener-

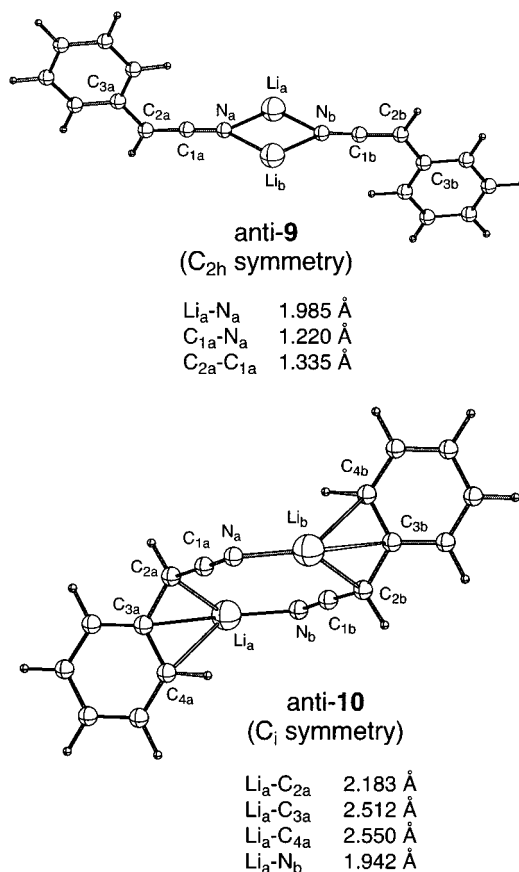
(19) Koch, R.; Anders, E. *J. Org. Chem.* **1994**, *59*, 4529-4534.(20) Abbotto, A.; Streitwieser, A.; Schleyer, P. v. R. *J. Am. Chem. Soc.* **1997**, *119*, 11255-11268.

Chart 4. Possible Constitutional Isomers of Cyclic Dimers of Lithiated Phenylacetonitrile^a^a *syn*-Isomers of 9–12 not shown.

gies at the 3-21G level and DFT energies at the B3LYP/6-31+G* level were determined (Table 3). As can be seen, the N-lithiated isomer **3**·(η^4 -12-crown-4) is predicted to be more stable than the C-lithiated isomer **6**·(η^4 -12-crown-4), matching the reported X-ray structure **A**. Note that the 3-21G//PM3 and B3LYP/6-31+G*//PM3 relative energies are quite similar, as they were for unsolvated **3** and **6** (Table 2). This observation suggests that the diffuse-function-augmented basis sets needed to adequately describe isolated anions^{21,22} are not essential for qualitative energy comparisons of species with “covalent” Li–N and Li–C bonds.

Modeling of Known N-Lithiated Homodimers B and C

The known homodimeric structures of lithiated phenylacetonitrile both adopt an N-lithiated dimer structure (**B** and **C** in Chart 3). A head-to-tail (C,N)-bridged dimer analogous to **8** should certainly be considered as a possible alternate connectivity. Such a structure (**F**, Chart 3) was demonstrated for lithiated 2,2-dimethylcyclopropyl nitrile in the solid state,⁶ and in this case the energetic penalty associated with placing a trigonal carbon in a cyclopropyl ring no doubt favors C-metalation. In total, seven cyclic dimer connectivities can be imagined for lithiated phenylacetonitrile: these are shown in Chart 4 as 9–15.

**Figure 2.** PM3 equilibrium geometries and selected bond lengths of unsolvated dimers *anti*-9 and *anti*-10.

Geometry optimizations at the PM3 level were then carried out, and minima for *anti*- and *syn*-diastereomers of 9–12 could be located (Figures 2 and 3).

C-lithiated dimer **13** could potentially exist in a total of 15 diastereomeric forms; each of these was constructed and submitted to geometry optimization. In the end only two of the potential fifteen C-lithiated dimer minima could be located (**13a,b**; see Figure S1 of the Supporting Information): nine starting geometries minimized to head-to-tail (C,N)-bridged dimers **10**, and four starting geometries minimized to head-to-head (C,N)-bridged dimers **11**. (C)(C,N)-bridged dimer **14** could exist in a total of six diastereomeric forms, but none of these minima could be located: three starting geometries minimized to head-to-head (C,N)-bridged dimer **11**, two to head-to-tail (C,N)-bridged dimer **10**, and one to (N)-(C,N)-bridged dimer **12**. Finally, none of the potential six diastereomeric forms of (C)(N)-dimer **15** could be located; all starting geometries minimized to (N)(C,N)-bridged dimer **12**. Key geometric parameters for *anti*-9–12 and their solvates (vide infra) are summarized in Tables S11–S14 of the Supporting Information. One feature worthy of note in (C,N)-bridged dimers *anti*-10–12 is the η^3 -coordination of the benzyl fragment, analogous to that observed in C-lithiated monomer **6** (cf. Figures 1–3).

As can be seen from Table 4, dimerization of **3** to 9–12 is predicted to be highly exothermic, with 3-21G//PM3 dimerization energies on the order of –55 to –62 kcal/mol.

PM3 and 3-21G//PM3 energies suggest that head-to-tail (C,N)-bridged dimers *syn*- and *anti*-10 would be the most stable constitutional isomers. At the 3-21G//PM3

(21) Spitznagel, G. W.; Clark, T.; Chandrasekhar, J.; Schleyer, P. v. R. *J. Comput. Chem.* **1982**, 3, 363–371.

(22) Clark, T.; Chandrasekhar, J.; Spitznagel, G. W.; Schleyer, P. v. R. *J. Comput. Chem.* **1983**, 4, 294–301.

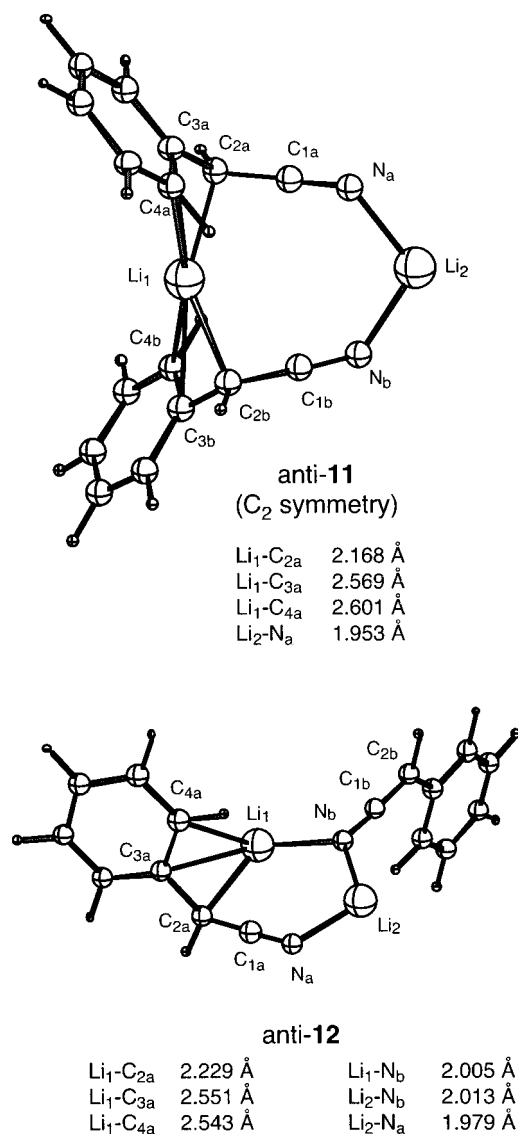


Figure 3. PM3 equilibrium geometries and selected bond lengths of unsolvated dimers *anti*-11 and *anti*-12.

level constitutional isomers **9**, **11**, and **12** are 4–6 kcal/mol higher in energy than *anti*-**10**, and C-lithiated dimers **13a,b** are quite unstable, being 42–44 kcal/mol higher in energy than *anti*-**10**. Clearly, as was found for monomeric lithiated phenylacetonitrile, the calculations of *unsolvated* dimers provide no insight as to why N-lithiated dimers **B** and **C** would be observed by X-ray crystallography and multinuclear NMR.

To determine whether the observation of **B** in the solid state could be attributed to the effects of solvation, bis-(η^2 -TMEDA) solvates of *anti*- and *syn*-**9**–**12** were constructed and subjected to PM3 geometry optimization and 3-21G single-point energy calculations. As noted earlier, Anders has shown that PM3 models well the structure of **B** (Table S11 in the Supporting Information).³ Interestingly, bis(η^2 -TMEDA) solvates of C-lithiated dimers **13a,b** could not be located; minimization led to rupture of the dimer structure. As can be seen in Table 4, PM3 energies would lead to the prediction of *syn*-**10** as the most stable constitutional isomer, in conflict with Boche's crystal structure of **B**⁵ and our previous multinuclear solution NMR studies.¹³ However, energies at the 3-21G//PM3 level correctly predict N-lithiated dimers **9** to be the

most stable. Since the 3-21G//PM3 energies of the bis-(η^2 -TMEDA) solvates of *anti*- and *syn*-**9** are nearly identical, it is likely that packing considerations are responsible for the pure *anti*-stereochemistry observed by Boche in the solid state. In solution it is quite likely that both diastereomers are present; we attribute the single set of ⁶Li, ¹³C, and ¹⁵N NMR resonances observed in toluene solution (0.1 M) at –90 °C to accidental equivalence or rapid *anti*–*syn* interconversion.¹³

Multinuclear NMR studies also demonstrated a cyclic N-lithiated dimer structure (**C**) for lithiated phenylacetonitrile at 0.1 M in 2:1 toluene/Et₂O solution at –90 °C. Since these studies did not provide any insight as to the solvation number at lithium, we constructed both bis(Et₂O) and tetrakis(Et₂O) solvates of *anti*-**9**–**13** and determined 3-21G//PM3 energies (Table 5).

Solvation of the dimers by two diethyl ether ligands is quite exothermic (–48 to –60 kcal/mol). However, further addition of two diethyl ether ligands is markedly less exothermic for **9** and **11**, and is slightly endothermic for **10** and **12** (incremental solvation energies –4.7 to +4.7 kcal/mol). Schleyer has estimated that sequential ethereal solvation of organolithium compounds is entropically unfavorable by 5–10 (cal/mol)/K.²⁰ At –90 °C coordination of two Et₂O molecules would therefore introduce a – ΔS term of +1.8 to +3.6 kcal/mol. On this basis we consider it likely that 0.1 M lithiated phenylacetonitrile would exist in 2:1 toluene/Et₂O as a disolvate, rather than a tetrasolvate. Note that three coordination for lithium is not unusual; many disolvated dimers of LiHMDS have been characterized by multinuclear NMR,²³ and three-coordinate lithium is often seen in solid-state structures of lithium alkoxides and amides.²⁴ However, no matter whether the di- or tetrasolvate is formed, 3-21G//PM3 energies predict that N-lithiated dimer *anti*-**9** would be the most stable constitutional isomer, consistent with NMR structure **C**. PM3 energies on the other hand suggest *anti*-**10** to be the most stable disolvate, and most stable tetrasolvate.

Historically, calculations on solvated organolithiums have often been “simplified” by using water as a model for diethyl ether or THF. To see the effect of this substitution on lithiated phenylacetonitrile, 3-21G//PM3 energies were determined for bis- and tetrakis(water) solvates of *anti*-**9**–**12**. As can be seen in Table 6, water is not a good model for diethyl ether.

First, unlike diethyl ether, incremental solvation energies for formation of the tetrasolvates are significant (–48 to –51 kcal/mol), suggesting facile formation of the tetrasolvate. This dichotomy is likely due to the small size of water relative to diethyl ether. Second, for both the bis- and tetrakis(water) solvates, head-to-tail (C,N)-bridged dimer *anti*-**10** is predicted to be the most stable, rather than the N-lithiated dimer **9** observed for the diethyl ether solvate. This interesting result suggests that very small solvents might effectively promote formation of head-to-tail (C,N)-bridged dimer **10**.

Review of metrical parameters for all the solvated dimers (Tables S11–S14 in the Supporting Information) reveals two interesting trends. First, in all cases, solvation of (C,N)-bridged dimers *anti*-**10**–**12** causes the

(23) Lucht, B. L.; Collum, D. B. *J. Am. Chem. Soc.* **1995**, *117*, 9863–9874.

(24) Pauer, F.; Power, P. P. In *Lithium Chemistry: A Theoretical and Experimental Overview*; Sapse, A.-M., Schleyer, P. v. R., Eds.; John Wiley & Sons: New York, 1995; pp 295–392.

Table 4. Relative Energies, Dimerization Energies, and Solvation Energies^a for Lithiated Phenylacetoneitrile Dimers 9–13 and Corresponding Bis(η^2 -TMEDA) Solvates

	unsolvated			bis(η^2 -TMEDA) solvates		
	PM3 energy	3-21G//PM3 energy	3-21G//PM3 dimerization energy	PM3 energy	3-21G//PM3 energy	3-21G//PM3 solvation energy
<i>anti</i> -9	6.71	4.91	−56.88	4.46	0.00	−90.15
<i>syn</i> -9	6.72	4.94	−56.85	4.40	0.19	−90.00
<i>anti</i> -10	0.15	0	−61.79	2.19	9.82	−75.43
<i>syn</i> -10	0.00	1.97	−59.82	0.00	15.06	−72.15
<i>anti</i> -11	1.00	4.30	−57.49	3.64	21.88	−67.67
<i>syn</i> -11	0.22	5.11	−56.68	3.99	25.52	−64.83
<i>anti</i> -12	7.60	5.93	−55.86	5.84	9.27	−81.90
<i>syn</i> -12	7.59	5.97	−55.82	4.53	11.84	−79.38
13a	31.13	42.58	−19.51	nl ^b		
13b	32.97	44.27	−17.52	nl ^b		

^a In kilocalories per mole. ^b Not located; geometry optimization led to disruption of the dimer structure.

Table 5. Relative Energies and Solvation Energies^a for Bis- and Tetrakis(diethyl ether) Solvates of Lithiated Phenylacetoneitrile Dimers 9–13

	bis(diethyl ether) solvates			tetrakis(diethyl ether) solvates		
	PM3 energy	3-21G//PM3 energy	3-21G//PM3 solvation energy	PM3 energy	3-21G//PM3 energy	3-21G//PM3 incremental solvation energy ^b
<i>anti</i> -9	4.17	0	−59.65	4.35	0.00	−4.52
<i>anti</i> -10	0	5.09	−49.65	0.00	12.92	3.30
<i>anti</i> -11	2.23	10.99	−48.06	5.75	10.81	−4.69
<i>anti</i> -12	5.44	5.69	−54.98	9.00	14.87	4.66
13a	44.22	48.77	−48.25			
13b	44.93	45.47	−53.54			

^a In kilocalories per mole. ^b Stabilization of the tetrasolvate relative to the disolvate.

Table 6. Relative Energies and Solvation Energies^a of Bis- and Tetrakis(water) Solvates of Lithiated Phenylacetoneitrile Dimers 9–13

	bis(water) solvates		tetrakis(water) solvates	
	3-21G//PM3 energy	solvation energy	3-21G//PM3 energy	incremental solvation energy ^c
<i>anti</i> -9	5.20	−71.89	5.20	−48.28
<i>anti</i> -10	0.00	−72.18	0.00	−48.28
<i>anti</i> -11	6.88	−69.60	4.00	−51.16
<i>anti</i> -12	5.98	−72.12	6.11	−48.15
13a	38.11	−76.38		
13b	nl ^b			

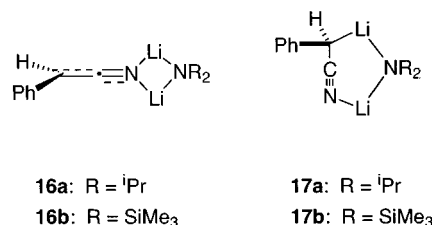
^a In kilocalories per mole. ^b Not located; reverted to *anti*-11.

^c Stabilization of the tetrasolvate relative to the disolvate.

benzyl group to “slip” from η^3 - to η^1 -coordination. Apparently ether and amine solvation is preferred to internal π -solvation by the phenyl ring. Second, whereas Li–N and Li–C bond lengths of the disolvated dimers differ little from that of unsolvated *anti*-9–12, Li–N and Li–C bond lengths in the tetrasolvated dimers (including the bis(η^2 -TMEDA) solvates) are typically 0.05–0.10 Å longer than those of the unsolvated dimers. These increased bond lengths are consistent with the notion that solvation renders the lithium atom less electrophilic.

Lithiated Phenylacetoneitrile/Amide Heterodimers D and E

Heterodimeric structures of lithiated phenylacetoneitrile with LDA (structure **D**) and LiHMDS (structure **E**) have also been characterized by X-ray diffraction⁷ and NMR spectroscopy, respectively.¹³ Unsolvated structures **16a,b** and hypothetical (N)(C,N)-bridged constitutional isomers **17a,b** were constructed and subjected to PM3 geometry optimization and 3-21G single-point energy calculations (Chart 5, Table 7).

Chart 5. Lithiated Phenylacetoneitrile/Amide Heterodimers

Association energies of lithiated phenylacetoneitrile with LDA and LiHMDS range from −55 to −63 kcal/mol, and are similar to the dimerization energies of lithiated phenylacetoneitrile to 9–12. As can be seen, the observed N-lithiated dimers **16a,b** are calculated to be 6.48 and 1.15 kcal/mol more stable than **17a,b**. The bis(η^2 -TMEDA) solvates were then constructed and optimized. As Anders reported earlier, the PM3 geometry of **16a**·2(η^2 -TMEDA) effectively reproduces the bond lengths and angles of the observed heterodimer **D**.³ Comparison of 3-21G//PM3 energies reveals that solvation enhances the energetic preference for N-lithiation of the nitrile, especially in the LiHMDS heterodimer **16b/17b**. Thus, 3-21G//PM3 energies of discrete solvates indicate strong preferences (13.74 and 24.41 kcal/mol, respectively) for the N-lithiated dimers, consistent with the observation of **D** and **E**.

Monomeric and Dimeric Lithiated Phenylacetoneitrile in THF Solution

The structure of lithiated phenylacetoneitrile in THF solution has received significant attention in the literature.^{4,13–17,25} In pure THF, freezing point depression

Table 7. Relative Energies, Association Energies, and Solvation Energies^a for Lithiated Phenylacetonitrile Heterodimers **16 and **17** and Their Bis(η^2 -TMEDA) Solvates**

	unsolvated			bis(η^2 -TMEDA) solvates		
	PM3 energy	3-21G//PM3 energy	3-21G//PM3 association energy	PM3 energy	3-21G//PM3 energy	3-21G//PM3 solvation energy
16a	5.32	0.00	−62.73	0.00	0.00	−36.31
17a	0.00	6.48	−56.24	6.85	13.74	−29.05
16b	0.00	0.00	−56.55	0.00	0.00	−44.29
17b	−3.09	1.15	−55.41	2.70	24.41	−21.04

^a In kilocalories per mole.**Table 8. Relative Energies and Solvation Energies^a of Bis- and Tetrakis(THF) Solvates of Dimers *anti*-**9**–**12****

	bis(THF) solvates		tetrakis(THF) solvates	
	3-21G//PM3 energy	solvation energy	3-21G//PM3 energy	incremental solvation energy ^b
<i>anti</i> - 9	0.00	−67.38	0.00	−36.37
<i>anti</i> - 10	1.46	−61.02	6.37	−31.45
<i>anti</i> - 11	10.41	−56.37	18.09	−28.68
<i>anti</i> - 12	3.62	−64.78	2.74	−37.25

^a In kilocalories per mole. ^b Stabilization of the tetrasolvate relative to the disolvate.

measurements at 0.087 M¹⁷ and acidity measurements below 1 mM²⁵ indicate a monomeric aggregation state. On the basis of changes in the CN region of the IR and Raman spectra of lithiated phenylacetonitrile, Wartski and Corset proposed a monomer–dimer equilibrium at 0.25 M in 30:70 THF/toluene,⁴ and exclusive monomer at 0.025 M in pure THF.¹⁵ These studies, important as they are, do not shed any light on constitutional isomerism. In our view, the most reliable indicator of connectivity in solution is the observation of scalar coupling (⁶Li–¹⁵N, ⁷Li–¹⁵N, or ⁶Li–¹³C). However, in THF solution we have not yet been able to observe scalar coupling in lithiated phenylacetonitrile or lithiated 1-naphthylacetonitrile.^{13,14} To rule out the possibility that the loss of coupling was due to formation of a separated ion pair, Reich's HMPA titration protocol²⁶ was applied. These studies (at 0.1 M in 3:2 THF/diethyl ether and 20:1 THF/hexane, at −135 °C)¹⁴ demonstrated that lithiated phenylacetonitrile exists in THF as a contact rather than separated ion pair. It thus seems likely that extremely fast chemical exchange is to blame for our previous failures to observe scalar coupling of ⁶Li and ⁷Li to ¹⁵N or ¹³C.

To address the issue of constitutional isomerism in THF solution, we therefore constructed explicit THF solvates of dimers *anti*-**9**–**12** and monomers **3** and **6**. As seen in Table 8, 3-21G//PM3 incremental solvation energies indicate facile formation of the tetrakis(THF) solvates of dimers *anti*-**9**–**12**.

As in the case of water (Table 6), the smaller size of THF relative to diethyl ether would appear to be responsible for the ease of attaining four-coordination at lithium. However, unlike the corresponding water solvates, the most stable bis(THF)- and tetrakis(THF) solvates are N-lithiated dimers *anti*-**9**. Regarding monomeric lithiated phenylacetonitrile, mono-, di-, and trisolvates of **3** and **6** could be located using PM3 geometry optimization (Table 9).

Although five-coordination was achieved by Li in 12-crown-4-solvate structure **A**, tetrakis(THF) solvates of **3**

and **6** could not be located; the fourth THF ligand always departs. Incremental THF solvation of N-lithiated isomer **3** causes little change in the PM3 geometry other than increased Li–N and Li–O bond lengths. For the C-lithiated isomer **6**, the mono(THF) solvate retains the η^3 -benzyl lithium structure seen in the PM3 geometry of unsolvated **6**. The di- and trisolvates however revert to a classical η^1 -structure similar to that seen for the 12-crown-4 solvate. HF (3-21G) and DFT (B3LYP/6-31+G*) geometry optimizations also indicate a classical η^1 -structure for the structure of **6**·3THF.

Using the PM3 geometries, both 3-21G and B3LYP/6-31+G* energies were calculated, and as can be seen in Table 9, incremental solvation energies are significant through the trisolvate. The B3LYP/6-31+G* incremental solvation energies are smaller than those based on the 3-21G basis set, but on the basis of these data, it would appear that lithiated phenylacetonitrile exists at high THF concentrations as the N-lithiated trisolvate. For the tris(THF) solvates of **3** and **6**, we note again that the energy difference does not significantly change as the level of the single-point calculation is raised from 3-21G to B3LYP/6-31+G* (cf. Tables 2 and 3 for unsolvated and 12-crown-4 solvates of **3** and **6**). Similarly, the energy difference between the C- and N-lithiated trisolvates is only slightly decreased at higher level HF (3-21G) and DFT (B3LYP/6-31+G*) geometries (Table 9). Therefore, we find no support for a recent proposal^{4,16} that monomeric lithiated phenylacetonitrile adopts a (C,N)-bridged structure in THF solution, and conclude instead that THF-solvated monomeric lithated phenylacetonitrile is N-lithiated.

The predicted THF solvation numbers of lithium in N-lithiated dimer **9** and monomer **3** deserve further comment. Whereas dimeric LiHMDS has been experimentally determined to form only mono(THF) and bis(THF) solvates,²³ our 3-21G//PM3 calculations suggest that *anti*-**9** can easily form the tetrakis(THF) solvates (Table S7, Supporting Information). This dichotomy may be resolved by considering the low steric demand of the phenylacetonitrile unit in N-lithiated dimer **9**, relative to the large steric demand of hexamethyldisilazide. Regarding the THF solvation numbers in the corresponding monomers, Collum has experimentally determined an average THF solvation number of 3.0 ± 0.1 for monomeric LiHMDS at −20 °C, and 3.6 ± 0.2 at −80 °C.²³ Following the logic above, it would seem reasonable that the lower steric demand of the N-lithiated phenylacetonitrile unit relative to hexamethyldisilazide might make it possible to locate the tetrasolvate of **3**. Our inability to locate such a structure suggests that the PM3 method may overestimate steric effects, or that Collum's LiHMDS results reflect the presence of a secondary solvation shell.

(26) Reich, H. J.; Borst, J. P.; Dykstra, R. R.; Green, D. P. *J. Am. Chem. Soc.* **1993**, *115*, 8728–8741.

Table 9. Relative Energies,^a Incremental Solvation Energies, and PM3 Geometric Parameters for THF Solvates of Monomers **3 and **6****

	N-lithiated isomer 3			C-lithiated isomer 6		
	·1THF	·2THF	·3THF	·1THF	·2THF	·3THF
3-21G//PM3 energy	0.00	0.00	0.00	11.48	6.31	10.88
incremental solvation energy ^b	-36.52	-23.38	-20.12	-36.19	-28.54	-15.56
B3LYP/6-31+G*//PM3 energy	0.00	0.00	0.00	9.85	6.88	10.19
incremental solvation energy ^b	-24.37	-13.98	-11.81	24.43	-16.95	-8.50
3-21G//3-21G energy			0.00			6.83
B3LYP/6-31+G*//B3LYP/6-31+ G*			0.00			6.75
bond lengths (Å)						
Li-N	1.800	1.838	1.889	4.125	3.653	3.838
C1-N	1.203	1.198	1.195	1.166	1.168	1.169
C1-C2	1.345	1.349	1.353	1.416	1.422	1.419
Li-C2				2.069	2.094	2.159
Li-C1				3.105	2.767	2.918
Li-C3				2.427	2.883	2.971
Li-C4				2.475	3.535	3.550
Li-O	1.964	1.976	2.063	1.962	2.011	2.078
		1.985	2.057		2.001	2.060
			2.035			2.041
bond angles (deg)						
C2-C1-N	178.3	178.8	178.3	178.2	178.6	178.8
C1-N-Li	177.8	167.0	177.4			
Li-C1-C2				33.1	47.7	44.9
Li-C2-C3				84.9	107.0	108.9

^a All energies in kilocalories per mole. ^b Stabilization resulting from each sequential solvation event.

Chart 6. 3-21G//PM3 Dimerization Enthalpies of Various Solvates

	ΔH (kcal/mol)
2 (3·TMEDA) \rightleftharpoons anti-9·2TMEDA	-35.7
2 (3·3Et ₂ O) \rightleftharpoons anti-9·4Et ₂ O + 2 Et ₂ O	-24.2
2 (3·3THF) \rightleftharpoons anti-9·4THF + 2 THF	-0.60

Modeling of Observed Aggregation States

As a final test of the reliability of the 3-21G//PM3 protocol in predicting structures of lithiated phenylacetonitrile, we consider the dimerizations shown in Chart 6.

First, mono(TMEDA) solvates of **3** and **6** were obtained by PM3 geometry optimizations and their 3-21G energies calculated (Table S10, Supporting Information). The most stable TMEDA-solvated monomer was 3·(TMEDA), and the dimerization of this species is predicted to be quite exothermic (-35.7 kcal/mol). This calculation matches our NMR observation of only dimer **9** at [Li] = 0.1 M in toluene in the presence of 1 equiv of TMEDA.¹³

Second, the aggregation state of 0.1 M lithiated phenylacetonitrile in 2:1 toluene/diethyl ether was addressed. Since the concentration of diethyl ether in this case is approximately 3.2 M, mono-, di-, and trisolvates of **3** and **6** were located. In all cases **3** is the most stable, and not surprisingly, solvation by the third diethyl ether is only slightly exothermic (-3.48 kcal/mol, Table S9, Supporting Information). Dimerization of 3·3Et₂O to anti-9·4Et₂O with release of two molecules of bound solvent is predicted to be exothermic by -24.2 kcal/mol (Chart 6). This is only one of four reasonable dimerization processes. In order of increasing exothermicity, the others are (a) 2(3·3Et₂O) to anti-9·2Et₂O + 4Et₂O (-19.7 kcal/mol), (b) 2(3·2Et₂O) to anti-9·2Et₂O + 2Et₂O (-26.6 kcal/mol), and (c) 2(3·2Et₂O) to anti-9·4Et₂O (-31.2 kcal/mol). The high exothermicities of these dimerizations are quite consistent with our NMR observation of dimer **9** as the major species in the presence of a large excess of diethyl ether.¹³

Last, we address the aggregation state of lithiated phenylacetonitrile in THF solution. As discussed earlier, the most reasonable species to consider are 3·3THF and 9·4THF. In contrast to the cases discussed above, dimerization (with liberation of two bound THF molecules) is predicted to be almost thermoneutral (-0.60 kcal/mol). On the basis of Fraenkel's study of an analogous monomer-dimer equilibrium of neopentylolithium in THF,²⁷ this dimerization process would be entropically favored by approximately 11 (cal/mol)/K. At -90 °C the free energy change for the dimerization can thus be estimated at -2.6 kcal/mol. This slightly exergonic result would therefore implicate a [THF]-dependent monomer-dimer equilibrium, which is exactly what has been proposed by Wartski and Corset on the basis of IR and Raman spectroscopy in THF/toluene solvent mixtures.⁴ With increasing concentrations of THF, mass action would eventually favor exclusive formation of monomer, a prediction confirmed by freezing point depression¹⁷ and acidity²⁵ measurements in pure THF.

Conclusion

Numerous computational studies by other workers have addressed the effects of solvation on organolithium structure and reactivity.^{20,28-33} The present study is the first to illustrate the dominant role of solvation in ordering the energies of competing N- and C-metalated

(27) Fraenkel, G.; Chow, A.; Winchester, W. R. *J. Am. Chem. Soc.* **1990**, *112*, 6190-6198.

(28) Romesberg, F. E.; Collum, D. B. *J. Am. Chem. Soc.* **1994**, *116*, 9187-9197.

(29) Romesberg, F. E.; Collum, D. B. *J. Am. Chem. Soc.* **1995**, *117*, 2166-2178.

(30) Thompson, A.; Corley, E. G.; Huntington, M. F.; Grabowski, E. J. J.; Remenar, J. F.; Collum, D. B. *J. Am. Chem. Soc.* **1998**, *120*, 2028-2038.

(31) Nilsson Lill, S. O.; Arvidsson, P. I.; Ahlberg, P. *Tetrahedron: Asymmetry* **1999**, *10*, 265-279.

(32) Piffil, M.; Weston, J.; Günther, W.; Anders, E. *J. Org. Chem.* **2000**, *65*, 5942-5950.

(33) Amedjkouh, M.; Pettersen, D.; Nilsson Lill, S. O.; Davidsson, Ö.; Ahlberg, P. *Chem.-Eur. J.* **2001**, *7*, 4368-4377.

constitutional isomers of a lithiated nitrile. As we have discussed, calculations of solvent-free monomers and dimers of lithiated phenylacetone nitrile, even at relatively high levels of theory, provide little insight into experimentally determined structures of *solvated* lithiated phenylacetone nitrile. However, calculations of *explicit solvates*, using HF energies, a small basis set without polarization functions (3-21G), and low-level semiempirical PM3 geometries, accurately model the experimentally observed structures. Selected single-point energy calculations at higher levels of theory, and geometry optimizations at the HF and DFT levels, reproduce these findings (Tables 2, 3, and 9), but require greatly increased computation time.

To review, N- and C-lithiated monomers **3** and **6** are nearly equal in energy at the 3-21+G**/3-21+G*, 6-31G**/6-31G*, and B3LYP/6-31+G**/6-31G* levels. However, solvation by 12-crown-4 stabilizes the N-lithiated constitutional isomer by 6.8 kcal/mol (3-21G//PM3 and B3LYP/6-31+G**/PM3), consistent with the observation of structure **A** by X-ray crystallography. Similarly, calculations of unsolvated dimers provide no insight into the experimentally observed dimer structures. On the basis of 3-21G//PM3 energies, the most stable unsolvated dimers are head-to-tail (C,N)-bridged dimers *anti*- and *syn*-**10**. However, 3-21G//PM3 calculations on the explicit TMEDA and diethyl ether solvates give N-lithiated dimers **9** as the most stable constitutional isomers, consistent with the observations of **B** and **C** by X-ray crystallography⁵ and multinuclear NMR.¹³ 3-21G//PM3 energies also correctly predict N-lithiated dimer structures for lithiated phenylacetone nitrile/amide heterodimers **D**⁷ and **E**.¹³

Why does solvation play such a significant role in ordering the energies of monomeric and dimeric constitutional isomers? It would appear that differing steric accessibility of the lithium atom in the constitutional isomers is an important factor. The N atom in N-lithiated monomer **3** represents a remarkably small amide ligand, and exerts little steric demand compared to the η^3 - or η^5 -organic fragment of C-lithiated monomer **6**. Similarly, among cyclic dimers **9**–**12**, the lithium atoms of **9** appear most sterically accessible to solvation. This steric model would suggest that solvation energies of dimers **9**–**12** would be most different for “large” solvents, and might be approximately equal for “small” solvents. Consistent with this idea, TMEDA and bis(diethyl ether) solvation of **9** is 10–15 kcal/mol more exothermic than that of **10**, but bis- and tetrakis(water) solvation energies for **9** and **10** are nearly identical.

These calculations provide renewed impetus for structural investigations of lithiated nitriles. Intriguing theoretical predictions include a preference for head-to-tail (C,N)-bridged dimer **10** both in donor-free media (Table 4) and in the presence of sterically undemanding ether solvents (Table 6). NMR experiments to characterize such species are under way.

Calculation Methods

Analytical geometry optimizations and single-point energy calculations at the PM3, 3-21G, and 6-31G* levels were performed using MacSpartan Pro (Wavefunction). DFT single-point energies (B3LYP/6-31+G**/PM3) were calculated out using Titan (Wavefunction); when necessary, the gvb-diis SCF convergence scheme was employed. DFT geometry optimizations (B3LYP/6-31+G**/B3LYP/6-31+G*) of **3**·3THF and **6**·3THF were performed using Gaussian 98 on a 160 MHz IBM 16-processor SP: each of these calculations required three weeks, running parallel on eight nodes. Particular care was taken to optimize equilibrium geometries of the explicit solvates. Extensive visual inspections and bond length and angle comparisons were made among competing constitutional isomers to ensure that the most favorable bound solvent conformations were obtained. All 82 optimized geometries were characterized as minima by vibrational frequency analysis (no imaginary frequencies). Selected ZPVE corrections (frequency scaling of 0.91) were performed for the PM3 and 3-21G geometries; in no case did the correction change relative energies by more than 0.8 kcal/mol. Solvation energy was calculated by comparing the absolute energy of a particular solvate to the sum of the absolute energies of the corresponding unsolvated structure and the appropriate number of unbound solvent molecules.

Acknowledgment. P.R.C. thanks Professors Daniel Crawford and James Tanko for helpful discussions and Professor Tanko for the use of Titan. J.D.M. thanks Orlando Acevedo for assistance with the DFT geometry optimizations and Professor Jeffrey D. Evansek for the use of his 16-processor IBM SP. Financial support was provided by the Jeffress Foundation and the Department of Chemistry, Virginia Tech.

Supporting Information Available: Absolute energies of all calculated structures, metrical parameters for **3**·3THF, **6**·THF, *anti*-**9**–**12** and their solvates, and **13a,b** and coordinates of all 82 optimized structures in pdb format. This material is available free of charge via the Internet at <http://pubs.acs.org>.